

Characterization of Ceramides with Phytosphingosine Backbone by Hydrogen-deuterium Exchange Mass Spectrometry

Irena Dapic,^{1,*} Lidija Brkljacic,² Ivone Jakasa,³ Renata Kobetic⁴

¹ International Centre for Cancer Vaccine Science, University of Gdansk, Gdansk, Poland

² Laboratory for Biomimetic Chemistry, Division of Organic Chemistry and Biochemistry, Ruđer Bošković Institute, Zagreb, Croatia

³ Laboratory for Analytical Chemistry, Department for Chemistry and Biochemistry, Faculty of Food Technology and Biotechnology, University of Zagreb, Zagreb, Croatia

⁴ Laboratory for Biomolecular Interactions and Spectroscopy, Division of Organic Chemistry and Biochemistry, Ruđer Bošković Institute, Zagreb, Croatia
Author's e-mail address: irena.dapic@ug.edu.pl

RECEIVED: February 27, 2019 * REVISED: October 1, 2019 * ACCEPTED: October 1, 2019

Abstract: Ceramides are a lipid subclass of the sphingolipids that show large structural diversity. Structural characterization of the ceramides (CERs) can lead to better understanding of their role and function in the biological system. Here we investigated representatives of NP (CER III, CER IIIB) and AP ceramide classes (CER VI) that contain phytosphingosine (P) backbone. Ceramides were characterized in positive ionization mode by hydrogen-deuterium exchange mass spectrometry (HDX-MS). Fragmentation in positive ionization mode of the CER III and CER VI resulted in abundant ions assigned to phytosphingosine moiety at m/z 282, 300 and 318. HDX-MS of fragments showed increase in m/z of corresponding ions confirming the exchange of deuterium. In negative ionisation spectra multiple fragment ions were assigned to fatty acyl (RCOO⁻) moiety. Presence of RCOO⁻ allowed unambiguous identification of CER III and CER IIIB which were distinguished by the presence of double bond on fatty acyl chain.

Keywords: Ceramide, sphingolipid, ESI-MS, tandem mass spectrometry, H-D exchange.

1. INTRODUCTION

SPHINGOLIPIDS represent an important group of molecules involved in key metabolic and structural functions in organism.^[1] Ceramides (CER) are complex group of sphingolipids consisting of sphingoid base linked by amide bond to fatty acid moiety.^[2] Their diversity and importance has been recognized in various biological pathways and particularly great diversity of CER is present in the outer most part of the skin, *stratum corneum* (SC).^[3–6] Together with cholesterol and free fatty acids, CERs are one of the main lipid classes in SC with more than several hundred individual CER species present.^[7–9]

CER present in SC were analyzed by thin layer chromatography (TLC),^[10–12] traditionally; however, TLC does not provide structural information of CERs which is necessary in some studies. Mostly used technique today

for detection of CERs is liquid chromatography coupled to mass spectrometry (LC-MS).^[13,14]

Capability of MS to provide structural information of CER is considered as advantage over other techniques since CERs might also be detected as positively or negatively charged species.^[15] CERs are most commonly analyzed by ESI and atmospheric pressure chemical ionisation (APCI), eventhough shotgun and matrix assisted laser desorption/ionisation (MALDI) techniques are also reported.^[16] Scherer et al. used hydrophilic interaction chromatography-MS (HILIC-MS) for direct profiling of hexosylceramide, lactosylceramide, sphingosine, sphinganine, phyto-SPH, di- and trimethyl-SPH, sphingosylphosphorylcholine, ceramide-1-phosphate, and dihydroceramide-1-phosphate and achieved base separation of all sphingolipid classes within 2 min.^[17] Using reversed phase liquid chromatography (RP-LC) t'Kindt et al.^[4] established analytical

platform for separation of majority of CER classes in SC with distinction of position and skeletal isomers of CERs. Collected data were used for formation of accurate mass retention time library for targeted profiling of the CERs in the skin. In another study, Sahle et al.^[18] developed LC-ESI-MS method for quantitation of [NP]-*d*₃-18 CER. Synthesized deuterated CER was used to enable analysis of permeability profile of exogenous [NP] in the skin. Raith et al. detected CERs in positive ionisation mode as occurring [M+H]⁺ and [M+Na]⁺ species and the quantification was performed in single ion monitoring (SIM) mode. Elution of *N*-stearoyl-phytosphingosine showed double peak which was referred to the diastereomeres present in (semi)synthetic ceramides.^[13] Product ions in negative ionisation mode of *N*-stearoylphytosphingosine were fragments that contained sphingoid base chain or the fragments formed after loss of neutral molecule (water, methanol).^[13]

1.1. Structural Characterization of CERs by Mass Spectrometry

Tandem mass spectrometry used for the structural characterization of the various CER classes has been carried out with several MS analyzers as linear ion trap,^[19–21] triple quadrupole^[22] or QTOF.^[4,23] Characterization of the CER using linear ion trap^[19] provided the specific fragment information for acyl and sphingoid unit of the N, NS, NdS and NH type of the ceramide. Obtained MS/MS library was used for the characterization of the N-type ceramides in the human SC. CERs from the SC were identified in negative ionization mode using chip-based direct infusion nanoelectrospray tandem MS revealing structures of fatty acyl and amide moieties. In another study, Hsu et al. showed unique fragmentation patterns after cleavage of C2-C3 bond belonging to fatty acid carboxylate anions (RCOO⁻) by collision induced dissociation (CID) of *N*-acylaminoethanol.^[24]

Hydrogen-deuterium exchange (HDX) is one of the techniques widely used for studying macromolecular interactions,^[25] protein conformation and dynamics^[17] or structural characterization.^[26,27] Studies showed that CERs influenced physical properties of the lipid bilayers and their structural organisation.^[28,29] Binding and interaction of the small molecules such as lipids may have large influence on the conformational state and the function, especially in the specific cases of the membrane and the transmembrane proteins.

Therefore, the aim of the present study was to elucidate the CERs structure using HDX-MS. For this purpose, CERs and phytosphingosine were characterized in positive ionisation mode and H-D exchange was confirmed by the tandem mass spectra on several structure sites. CERs were also characterized in the negative ionisation mode in

order to obtain more information on acyl chain structure. HDX-MS characterization of CERs is important for studies of dynamics of the SC environment and predictions of the possible penetration of the CER-containing cosmetic products in the skin.

2. EXPERIMENTAL

2.1. Materials

Ceramides III, IIIB, VI and phytosphingosine (P) were obtained from Evonik, HPLC grade methanol (MeOH) and EtOH-*d*₆ were purchased from Sigma-Aldrich and HPLC grade acetonitrile (ACN) was from Panreac. Stock solution of each CER was prepared in MeOH at concentration level of 1 mg/mL.

2.2. LC-ESI-MS/MS

CERs were analyzed on LC-MS system consisted of Agilent Technologies 1200 series HPLC system equipped with a binary pump, a vacuum membrane degasser, autosampler and injector interfaced with 6410 triple quadrupole mass spectrometer (QQQ) with electrospray ionisation source (ESI) (Agilent Technologies Inc., Palo Alto, CA, USA).

ESI-MS/MS analysis was conducted in positive and negative ionisation mode and LC-ESI-MS/MS was conducted in positive ionisation mode using multiple reaction monitoring (MRM). Capillary voltage was 2500 V, desolvation gas temperature was 350 °C and flow rate of 6 L/min, dwell time was 10, nebuliser pressure 13 psi, *m/z* range 10–2200. Fragmentor voltage was 135 V and collision energy used was 20 eV. For data acquisition and analysis Mass Hunter software (Agilent Technologies, Inc. 2006–2007) was used.

CER III, IIIB and VI were separated on chromatographic column Synergi Hydro-RP (Phenomenex, Torrance, CA, USA) guarded by Eclipse XDB-C18 precolumn (Agilent, Santa Clara, CA, USA) using gradient elution of mobile phase A (MilliQ water and 0.1 % HCOOH) and mobile phase B (MeOH) at flow rate of 0.5 mL/min. Elution gradient consisted of 95–100 % solvent B (0 to 5 min), 100 % solvent B (5–27 min) and 100–95 % solvent B (27 to 27.1 min). CERs were detected in positive ionisation mode using optimized MRM transitions for CER III 584→282 and 584→566; CER IIIB 582→282 and 584→564 and for CER VI 600→282 and 600→582.

3. RESULTS AND DISCUSSION

3.1. ESI-MS/MS Structural Characterization in Positive Ionisation Mode

CERs are important building blocks of the SC and also play a significant role in cellular metabolism. CERs in the skin

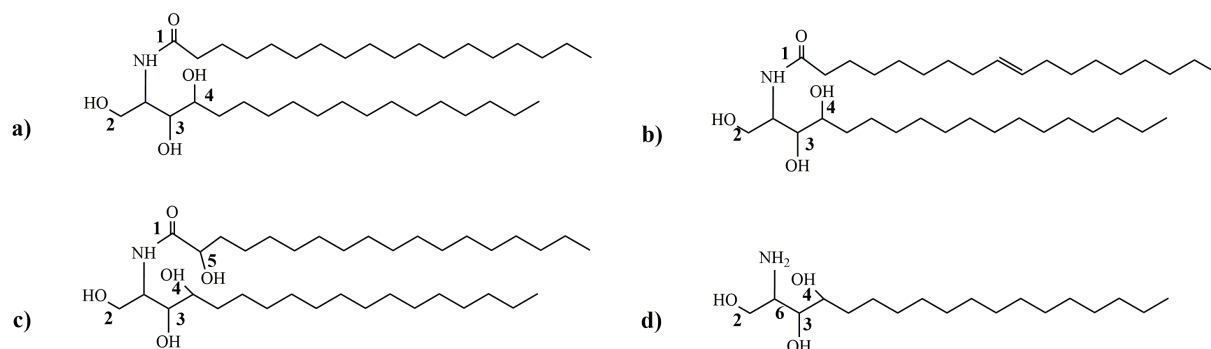


Figure 1. Structures of a) CER III, b) CER IIB, c) CER VI and d) phytosphingosine (P) used in this study.

have large range of sphingoid base and fatty acyl chain lengths which makes their identification challenging.^[30] Investigation of the CER organization within the biological environment has important role in the study of the skin barrier function, and studies have reported alteration of the CERs composition in impaired human and canine skin barrier.^[31,32] To address CERs complexity researchers are continuously seeking for methods convenient to reveal mechanisms of biomolecular interactions in the cells. To use advantage of sensitivity and specificity of MRM methods in some studies semi-quantification and profiling of the CERs performed with scheduled-MRM approach resulted with detection of more than 1000 CER species.^[9]

We have focused on structural analysis of synthetic CER III, CER IIB, CER VI and P to get better insight into the CER structure in this work. While CER III and CER IIB differ in the double bond presence on position C9 of the acyl chain, CER VI possesses α -hydroxy group on acyl chain (Figure 1, a, b, c). To obtain more detailed insight into the fragmentation of the sphingoid backbone, we used phytosphingosine (P) which is sphingoid base of the above mentioned investigated CERs (Figure 1, d).

In positive ionisation mode ESI-MS spectra showed peaks at m/z 584, m/z 582 and m/z 600 (not shown) which were assigned as protonated molecular ions for CER III, CER IIB and CER VI, respectively. CID product ion ESI-MS/MS spectra for CER III at CE 20 eV is shown in Figure 2, a. Further inspection of product ion spectra for all CERs shows $[M+H-H_2O]^+$ species formed after the nonspecific loss of one molecule of water from molecular ion (product ions at m/z 566, 564 and 582 for CER III, CER IIB and CER VI, respectively). Increasing CE to 20 eV for CER III and CER IIB, and 30 eV for CER VI yielded fragments formed due to the elimination of one (m/z 566, 564 i 582) or two (m/z 548, 546 and 564) molecules of water (CID generated product ion spectra at different energies for CER VI are shown in Supplementary Figure 1). The fragmentation spectra of CER III, CER IIB and CER VI also show fragments at m/z 318 that correspond to phytosphingosine moiety formed after amide bond cleavage (Figure 1, position 1). Applying the CE 20 eV results with triplet of product ions at m/z 300, 282 i 264 formed by elimination of the water from P (Figure 1., position 2, 3, 4) which can be seen from fragmentation spectra (Figure 2, b). Similar CID fragmentation pattern

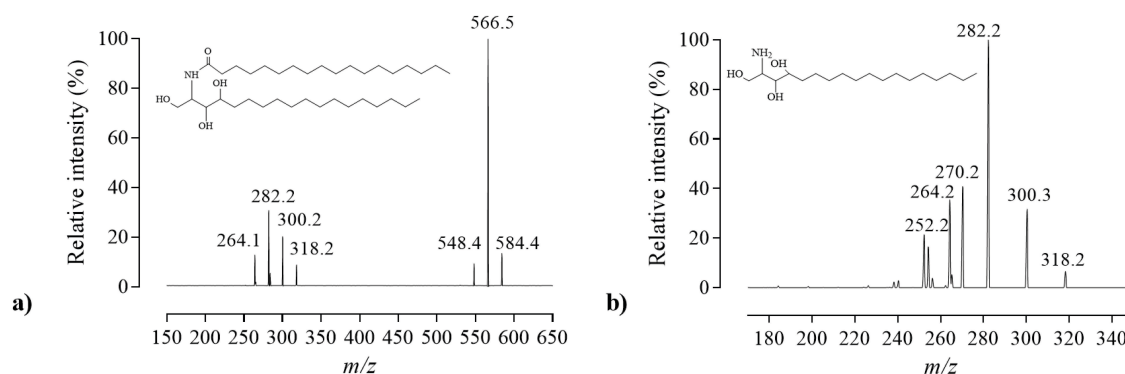


Figure 2. CID product ion ESI-MS/MS spectra in positive ionisation mode for: a) m/z 584 (CER III), CE 20 eV; b) m/z 318 (P), CE 20 eV.

(signals at m/z 300, 282 and 264) was observed at CE of 20 and 30 eV for CER III, CER IIIB and CER VI which indicates loss of water from sphingoid base building block of CERs. It is important to state that the increase of the CE did not change the cleavage mechanisms.

3.2. Hydrogen-deuterium Exchange of the Phytosphingosine and CER VI

Hydrogen-deuterium exchange MS (HDX-MS) is a powerful method for elucidating structure of the compounds. Isotope labeling of the CER by the exchange of the hydrogens resulted in mass shift of the molecular and product ions in mass spectra. This information can be used to unambiguously assign fragment ions and resolve ceramide structure. To investigate their fragmentation, CERs were dissolved in EtOH- d_6 , and further CID was obtained on triple quadrupole mass spectrometer. Results showed that after incubation of P, CER III, CER IIIB and CER VI in EtOH- d_6 , H-D exchange occurred (full scan ES+ spectra shown for P in Supplementary Figure 2).

Results showed that after dissolving P in EtOH- d_6 (P-HDX) there was an increase in m/z for the molecular ion and the corresponding product ions. The product ions of 319 at m/z 301 and 300 correspond to loss of one water $[M+H-H_2O]^+$ and $[M+H-DHO]^+$, respectively (Figure 3, a). Further elimination of the water at m/z 283 and 282 corresponds to loss of $[M+H-2H_2O]^+$ and $[M+H-DHO-H_2O]^+$, respectively. Loss of water yielded m/z 265 and 264 for the fragments $[M+H-3H_2O]^+$ and $[M+H-DHO-2H_2O]^+$, respectively. CID fragmentation of molecular ions at m/z 318 (m/z 60), 319 (m/z 60 and 61) and 320 (m/z 60, 61, 62) showed fragments ions with increasing m/z which could indicate exchange of the protons with deuterium (Figure 3).

Similar fragmentation pattern was showed for CER VI-HDX dissolved in EtOH- d_6 (Figure 4). Results showed that after dissolving in EtOH- d_6 (CER VI-HDX) there was an increase in m/z values of molecular ions and corresponding product ions compared to the product ion spectra of CER VI. Tandem mass spectra of protonated molecular ion (CER VI-HDX) at m/z 601 resulted in product ions at m/z 583 and 582 which correspond to loss of water in the form of $[M+H-H_2O]^+$ and $[M+H-DHO]^+$; furthermore, MS/MS of m/z 602 gave product ion spectra at m/z 584 and 583; and MS/MS of m/z 603 gave product ion spectra at m/z 584 and 585. Further, results showed that product ions at lower m/z values were formed after amide bond cleavage at position 1 (Figure 1, c) and elimination of the water. For protonated molecular ion of CER VI-HDX at m/z 601 this corresponded to the sphingoid base moiety at m/z 300 and 301 (after cleavage at position 1 and loss of H_2O and HDO), while for m/z 602 and 603 analogous signals were detected at corresponding m/z values (Figure 4). Moreover, tandem

mass spectra of molecular ion at m/z 603 showed product ions at m/z 62, 61 and 60 which may be analogous to the product ions generated after CID of P-HDX.

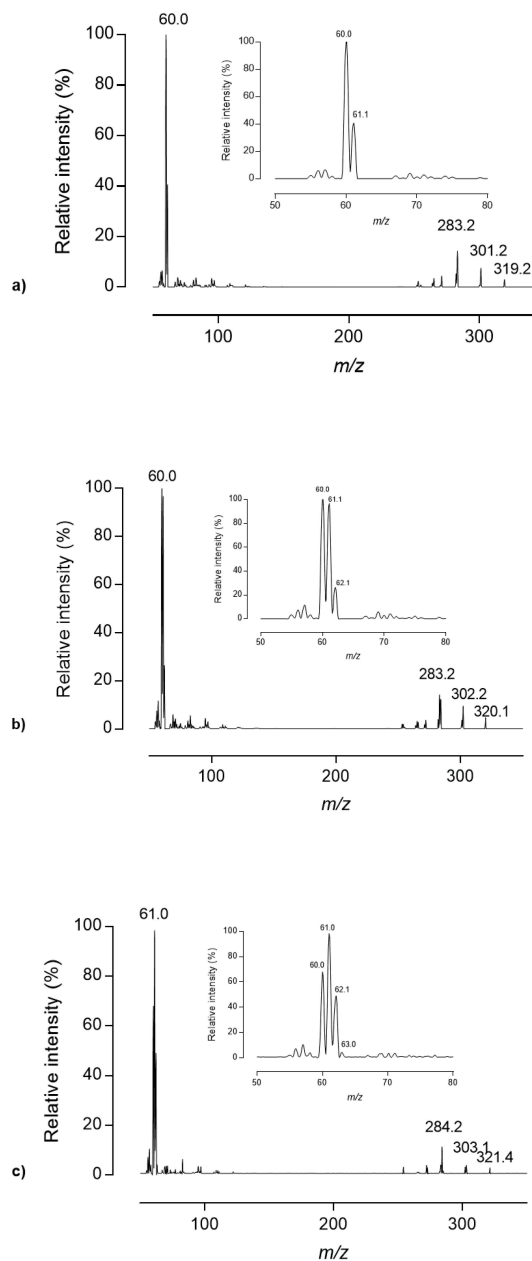


Figure 3. CID product ion ESI-MS/MS spectra in positive ionisation mode of P-HDX at: a) m/z 319, b) m/z 320, c) m/z 321. Inset shows the signals that correspond to cation fragment generated by CID which might be assigned as analogous ions corresponding to deuterium-labeled fragments at: a) m/z 60 and 61; b) m/z 60, 61, 62; c) m/z 60, 61, 62, 63. HDX spectra were obtained after dissolving phytosphingosine in EtOH- d_6 and used CE was 20 eV.

3.3. ESI-MS/MS Characterization of CER in Negative Ionisation Mode

While positive ionisation mode gives information on sphingoid base moiety, negative ionisation mode gives more insight into the structure of the acyl chain.^[24] CID in negative ionisation mode showed fragments which might be contributed to loss of water, fragments corresponding to fatty acid or to phytosphingosine moiety.

ESI-MS/MS spectra in negative ionisation mode for CER IIIB and CER VI showed molecular ions $[M-H]^-$ at m/z 580 and 598, respectively (Supplementary Figure 3). Product ions at m/z 544, 562 and 580 can be assigned to nonspecific loss of water at m/z 580 (CER IIIB) and m/z 598 (CER VI). In ESI-MS/MS spectra of CER III and CER IIIB ions at m/z 618 and 616 can be attributed to adduct $[M-H+2H_2O]^-$. This was evidenced by fragmentation of ion at m/z 618 with 5 eV CE which generated product ion at m/z 582 corresponding to $[M-H]^-$ of CER III (data not shown). Product ions of m/z 580 at CE to 25 eV showed fragments at m/z 324 and 267 which might be assigned as **f1** and **f4** for CER IIIB (Figure 5). Common product ion at m/z 267 for

CER IIIB and CER VI is assigned as fatty acid moiety after amide bond cleavage. Distinction of the product ion spectra of the CER VI from the CER IIIB is that corresponding fragment **f2** has signal at m/z 308 due to absence of double bond on C9 of acyl chain (Supplementary Figure 3, b). Fragment **f5** observed as signal at m/z 280 might be derived from dissociation of **f1** and loss of oxirane.^[24] Product ion **f3** observed as signal at m/z 281 is related to the fatty acid moiety and it is assumed to be generated via an intermediate.^[33] Rearrangement of **f1** and loss of H_2 can lead to formation of carboxyethanolamine anion (m/z 322) which is after rearrangement and loss of azirine suggested to generate fragment **f3** ($C_{17}H_{33}COO^-$) observed as signal at m/z 281.^[24] Product ion spectra in negative ionisation mode for molecular ions of CER IIIB and CER VI is shown in Supplementary Figure 3.

3.4. LC-MS Separation of CER III, CER IIIB and CER VI

CER are separated according to their hydrophobic properties and their retention on reversed phases column

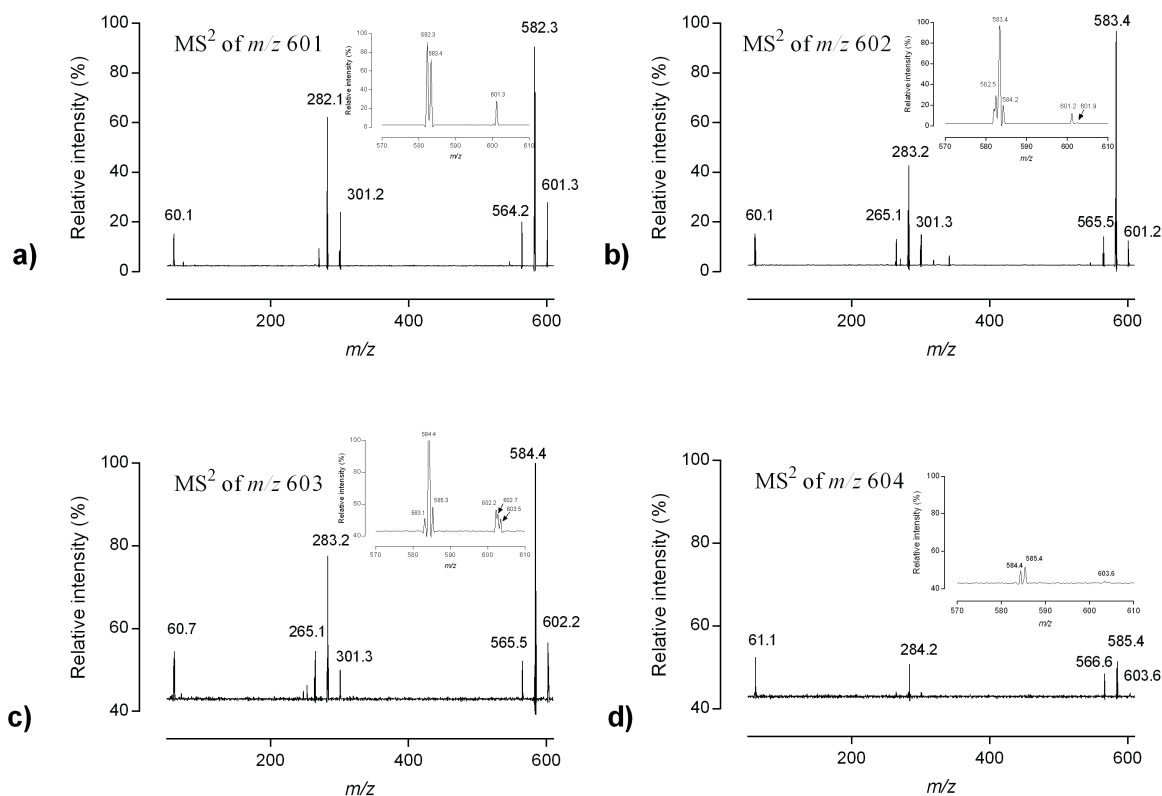


Figure 4. CID product ion spectra of CER VI-HDX at: a) m/z 601, b) m/z 602, c) m/z 603 and d) m/z 604. Increase in m/z of molecular ion corresponds to H-D exchange which is showed by increase in m/z of product ions. HDX was obtained after dissolving CER VI in $EtOH-d_6$ and CE was 20eV.

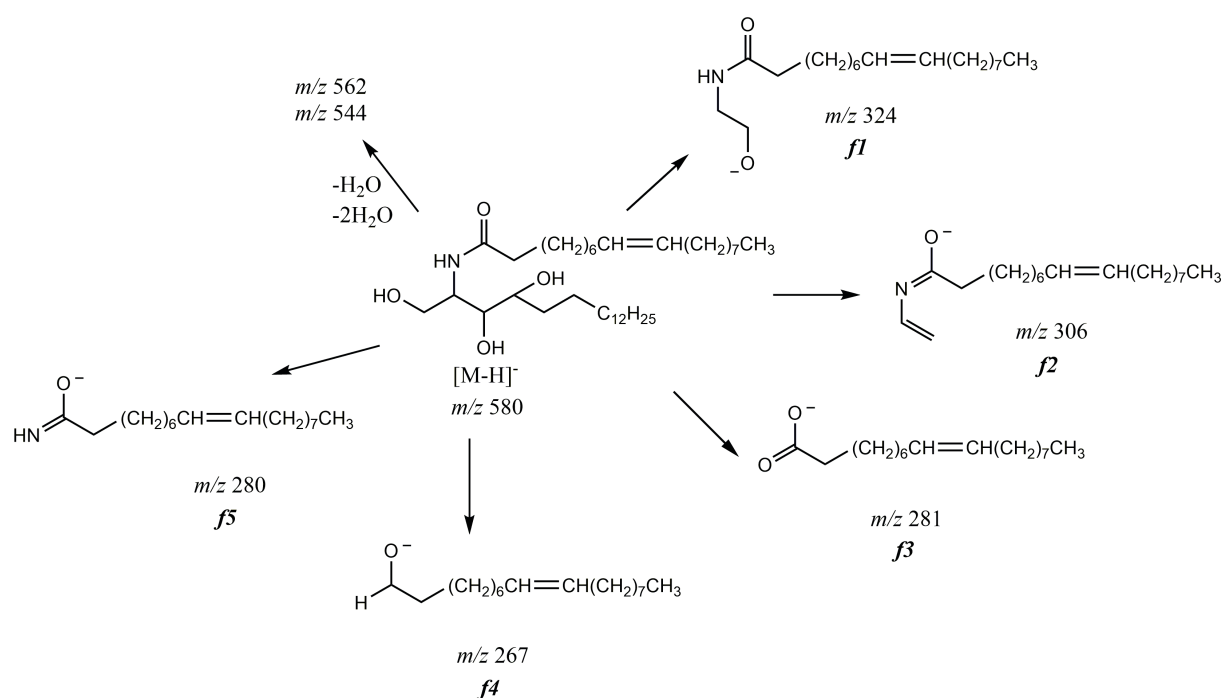


Figure 5. Fragmentation pathways for CER IIIB revealed from negative ionisation ESI-MS/MS spectra.

is affected by both, fatty acid and sphingoid base chain length as well as number of unsaturated bonds. Eventhough, CERs can be separated using both, normal and reversed phases, later might produce more efficient separation which is important especially when complex mixtures are analyzed. Synthetic CER III, CER IIIB and CER VI were separated on Synergi Hydro-RP chromatographic column using gradient mobile phase elution. CERs were detected using multiple reaction monitoring (MRM) for the transitions $[M+H]^+ \rightarrow 282$ and $[M+H]^+ \rightarrow [M+H-H_2O]^+$. MRM transition $[M+H]^+ \rightarrow 282$ showed higher signal intensity compared to $[M+H]^+ \rightarrow [M+H-H_2O]^+$ which can be appreciated from Supplementary Figure 4. Results showed double peaks of the CERs which can indicate different isomers of the CER present in the mixture affecting their retention times due to the interactions with the stationary phase.

4. CONCLUSION

The present study includes structural characterization of the CERs with the phytosphingosine backbone. Product ion spectra of $[M-H]^-$ showed distinct product ion spectra for CERs classes containing different fatty acyl moieties. Structure of the CERs was also investigated in positive ionisation mode by HDX-MS. Results suggested that H-D exchange occurred mostly on hydroxyl or amide moieties and this was confirmed by tandem mass spectra. HDX-MS

showed to be straightforward to perform low-cost alternative for obtaining isotope labeled CERs compared to commercially available isotope labelled products. Isotope labeling of CERs gives the better insight in their structure identification and the distinction from other endogenous compounds which potentially might be used in future skin research.

Acknowledgment. Authors would like to thank Dr Sanja Kezic for providing ceramide products.

Supplementary Information. Supporting information to the paper is attached to the electronic version of the article at: <https://doi.org/10.5562/cca3506>.

REFERENCES

- [1] H. Farwanah, T. Kolter, K. Sandhoff, *Biochim. Biophys. Acta - Mol. Cell Biol. Lipids* **2011**, *1811*, 854–860. <https://doi.org/10.1016/j.bbalip.2011.05.011>
- [2] J. Adams, Q. Ann, *Mass Spectrom. Rev.* **1993**, *12*, 51–85. <https://doi.org/10.1002/mas.1280120103>
- [3] J. van Smeden, L. Hoppel, R. van der Heijden, et al. *J. Lipid Res.* **2011**, *52*, 1211–1221. <https://doi.org/10.1194/jlr.M014456>
- [4] R. T'Kindt, L. Jorge, E. Dumont, et al. *Anal. Chem.* **2012**, *84*, 403–411. <https://doi.org/10.1021/ac202646v>

- [5] A. Hinder, C.E. Schmelzer, A. V. Rawlings, R. H. Neubert, *Skin Pharmacol. Physiol.* **2010**, *24*, 127–135. <https://doi.org/10.1159/000322303>
- [6] K. M. Joo, J. H. Hwang, S. Bae, et al. *J. Dermatol. Sci.* **2015**, *77*, 71–81. <https://doi.org/10.1016/j.jdermsci.2014.10.001>
- [7] Y. Masukawa, H. Narita, H. Sato, et al. *J. Lipid Res.* **2009**, *50*, 1708–1719. <https://doi.org/10.1194/jlr.D800055-JLR200>
- [8] Y. Masukawa, H. Narita, E. Shimizu, et al. *J. Lipid Res.* **2008**, *49*, 1466–1476. <https://doi.org/10.1194/jlr.M800014-JLR200>
- [9] G. P. Laffet, A. Genette, B. Gamboa, V. Auroy, J. J. Voegel, *Metabolomics* **2018**, *14*, 69. <https://doi.org/10.1007/s11306-018-1366-4>
- [10] J. M. Jungersted, L. I. Hellgren, T. Drachmann, G. B. E. Jemec, T. Agner, et al. *Skin Pharmacol. Physiol.* **2010**, *23*, 62–67. <https://doi.org/10.1159/000265676>
- [11] K. Shimada, J.-S. Yoon, T. Yoshihara, T. Iwasaki, K. Nishifuji, *Vet. Dermatol.* **2009**, *20*, 541–546. <https://doi.org/10.1111/j.1365-3164.2009.00847.x>
- [12] V. S. Thakoersing, J. van Smeden, A. a Mulder, J. *Invest. Dermatol.* **2012**, *133*, 59–67. <https://doi.org/10.1038/jid.2012.262>
- [13] K. Raith, R. H. Neubert, *Anal. Chim. Acta* **2000**, *403*, 295–303. [https://doi.org/10.1016/S0003-2670\(99\)00661-3](https://doi.org/10.1016/S0003-2670(99)00661-3)
- [14] K. Raith, S. Zellmer, J. Lasch, R. H. H. Neubert, et al. *Anal. Chim. Acta* **2000**, *418*, 167–173. [https://doi.org/10.1016/S0003-2670\(00\)00955-7](https://doi.org/10.1016/S0003-2670(00)00955-7)
- [15] E. Camera, M. Picardo, C. Presutti, P. Catarcini, S. Fanali, *J. Sep. Sci.* **2004**, *27*, 971–976. <https://doi.org/10.1002/jssc.200301712>
- [16] H. Farwanah, J. Wohlrab, R. H. H. Neubert, K. Raith, *Anal. Bioanal. Chem.* **2005**, *383*, 632–637. <https://doi.org/10.1007/s00216-005-0044-3>
- [17] M. Scherer, K. Leuthäuser-Jaschinski, J. Ecker, G. Schmitz, G. Liebisch, et al. *J. Lipid Res.* **2010**, *51*, 2001–2011. <https://doi.org/10.1194/jlr.D005322>
- [18] F. F. Sahle, S. Lange, B. Dobner, J. Wohlrab, R.H.H. Neubert, *J. Pharm. Biomed. Anal.* **2012**, *60*, 7–13. <https://doi.org/10.1016/j.jpba.2011.10.032>
- [19] J.-H. Shin, J. C. Shon, K. Lee, et al. *Anal. Bioanal. Chem.* **2014**, *406*, 1917–1932. <https://doi.org/10.1007/s00216-013-7601-y>
- [20] F.-F. Hsu, *Biochimie* **2016**, *130*, 63–75. <https://doi.org/10.1016/j.biochi.2016.07.012>
- [21] M.-H. Lin, J.H. Miner, J. Turk, F.-F. Hsu, *J. Lipid Res.* **2017**, *58*, 772–782. <https://doi.org/10.1194/jlr.D071647>
- [22] X. Han, *Anal. Biochem.* **2002**, *302*, 199–212. <https://doi.org/10.1006/abio.2001.5536>
- [23] S. Kirsch, M. Zarei, M. Cindrić, *Anal. Chem.* **2008**, *80*, 4711–4722. <https://doi.org/10.1021/ac702175f>
- [24] F.-F. Hsu, J. Turk, *J. Am. Soc. Mass Spectrom.* **2002**, *13*, 558–570. [https://doi.org/10.1016/S1044-0305\(02\)00358-6](https://doi.org/10.1016/S1044-0305(02)00358-6)
- [25] J. Cao, J. E. Burke, E. A. Dennis, *J. Biol. Chem.* **2013**, *288*, 1806–1813. <https://doi.org/10.1074/jbc.R112.421909>
- [26] M. E. Rerek, Chen, B. Markovic, et al. *J. Phys. Chem. B* **2001**, *105*, 9355–9362. <https://doi.org/10.1021/jp0118367>
- [27] G. F. Pirrone, R. E. Iacob, J. R. Engen, *Applications of Hydrogen/Deuterium Exchange MS from 2012 to 2014*, **2014**. <https://doi.org/10.1021/ac5040242>
- [28] B. Dutagaci, J. Becker-Baldus, J. D. Faraldo-Gómez, C. Glaubitz, *Biochim. Biophys. Acta* **2014**, *1838*, 2511–2519. <https://doi.org/10.1016/j.bbamem.2014.05.024>
- [29] B. Školová, A. Kováčik, O. Tesař, L. Opálka, K. Vávrová, *Biochim. Biophys. Acta - Biomembr.* **2017**, *1859*, 824–834. <https://doi.org/10.1016/j.bbamem.2017.01.019>
- [30] Z.-X. Jia, J.-L. Zhang, C.-P. Shen, L. Ma, *Anal. Bioanal. Chem.* **2016**, *408*, 6623–6636. <https://doi.org/10.1007/s00216-016-9775-6>
- [31] M. Janssens, J. van Smeden, G. S. Gooris, et al. *J. Lipid Res.* **2012**, *53*, 2755–2766. <https://doi.org/10.1194/jlr.P030338>
- [32] S. Chermrapai, F. Broere, G. Gooris, et al. *Biochim. Biophys. Acta - Biomembr.* **2018**, *1860*, 526–533. <https://doi.org/10.1016/j.bbamem.2017.11.013>
- [33] H. Farwanah, B. Pierstorff, C. E. H. Schmelzer, et al. *J. Chromatogr. B Anal. Technol. Biomed. Life Sci.* **2007**, *852*, 562–570. <https://doi.org/10.1016/j.jchromb.2007.02.030>